Available online at www.sciencedirect.com

ScienceDirect

Journal of the European Ceramic Society 26 (2006) 3919–3924

www.elsevier.com/locate/jeurceramsoc

Microstructure development and properties of novel Ba-doped phase Sialon ceramics

B. Basu[a,*], M.H. Lewis[b], M.E. Smith[b], M. Bunyard[b], T. Kemp[b]

[a] Department of Materials and Metallurgical Engineering, Indian Institute of Technology, Kanpur, India
[b] Centre for Advanced Materials, Department of Physics, University of Warwick, Coventry, UK

Received 20 October 2005; received in revised form 9 December 2005; accepted 6 January 2006
Available online 3 March 2006

Abstract

Herein, we report the microstructure and properties of the newly developed near monophasic S-Sialon ceramic, based on the composition of $Ba_2Si_{12-x}Al_xO_{2+x}N_{16-x}$ ($x = 20.2$). Appropriate amount of the precursor powders ($BaCO_3$, α-Si_3N_4, AlN, Al_2O_3) with a targeted composition of $BaAlSi_5O_2N_7$ was ball milled and hot pressed to full density in the temperature range of 1600–1750 °C for 2 h in nitrogen atmosphere. Extensive transmission electron microscopy (TEM) study has been conducted to understand the microstructure development and characterise the various morphological features in hot pressed S-Sialon. The sintering mechanism is based on the liquid phase sintering route, which involves the formation of a Ba–Al silicate liquid (<5%) with dissolved nitrogen at intergranular pockets. The experimental observation suggests that the S-phase crystallises in elongated platelet morphology with preferred growth parallel to the orthorhombic '*c*' axis and primary facet planes parallel to (1 0 0) and (0 1 0). The Ba-S-phase ceramic has an acoustically measured Young modulus of 210–230 GPa, a hardness of 13 GPa and a fracture toughness of 4 MPa m$^{1/2}$, little lower than typical of a ceramic with morphologically anisotropic grains contributing to bridging and pullout mechanisms.

Keywords: Microstructure; Mechanical Properties; Sintering; S-Sialon; Electron microscopy

1. Introduction

Several non-oxide ceramics, in particular silicon nitrides, owing to their high toughness and high temperature strength are intensively investigated and their potential applications are being explored. It is also well known that the improved thermo-mechanical properties can be obtained with a refined Sialon microstructure, a structure derived from Si_3N_4 with partial substitution of Si by Al and N by O.[1] Common engineering applications of this class of ceramics include ball bearing, cutting tool inserts, engine valves and several other tribological applications. In view of such potential applications, various mechanical[2,3] and tribological[4] properties were also investigated.

In the past two decades, Sialon ceramics, have been developed to a high level of microstructural control and Sialons are those based on the substituted forms of β and α-Si_3N_4, which derive their high modulus and hardness values from the rigid Si–N covalent framework as well as solid solution formation.[5–8] In addition to these intrinsic properties, it has been possible to develop moderate levels of fracture toughness (K_c) by increasing the fraction of large prismatic α′ or β′ crystals, which contribute to crack-bridging and pull-out mechanisms. Higher temperature properties may also be enhanced by appropriate control of residual phase constitution following liquid phase sintering.

The majority of engineering applications for β′/α′ ceramics remain in the lower temperature regime (generally less than 1000 °C) and a greater market penetration has been inhibited largely by economic factors. In view of this, a continuing quest exists for novel Sialon ceramics, which could be sintered at lowered temperatures and might be more tolerant to less expensive starting powders. Of the new phases that have been identified within M–Si–Al–O–N systems (M is a cation in Group II of the periodic table), many have comparatively high oxygen/nitrogen ratios, with reduced covalency and intrinsic properties, and those with high nitrogen content are difficult to sinter or to obtain with controlled phase content.[9] Early research identified the O′ phase (Al, O substituted derivative of Si_2N_2O) as being a competitor, but its pressureless sinterability is impaired by the small temperature tolerance between densification and decomposition (1650–1670 °C).[10] A recently discovered Sialon phase is the 'S

---

[*] Corresponding author. Fax: +91 512 2597505.
E-mail address: bikram@iitk.ac.in (B. Basu).

0955-2219/$ – see front matter © 2006 Elsevier Ltd. All rights reserved.
doi:10.1016/j.jeurceramsoc.2006.01.004

phase', having the composition of $M_2Al_xSi_{12-x}N_{16-x}O_{2+x}$ with $x \approx 2$, where M is a cation in Group II of the periodic table.[11] The larger cation (Ba/Sr) substitutes some of the Al/Si, and thus changes the possible compositions and the material properties. To date, research on this class of material is limited and only work, known to us, is the characterisation of Sr-doped S-phase using XRD and SEM–EDS.[11]

The discovery of S-phase[11,12] has motivated the present study to investigate sinterability and intrinsic properties in view of its relatively high nitrogen content. The structure is stabilised by divalent cations and has been analysed initially near to the composition of $M_2Si_{10}Al_{12}O_4N_{14}$ (M = Sr or Ba) although it may be prepared in less phase-pure form at lower levels of substitution (x) in a generic form $M_2Si_{12-x}Al_xO_{2+x}N_{16-x}$. In the present work, The Ba-containing S-phase ceramic is studied with an aim to illustrate the main features of microstructural evolution, because it is more readily sintered to the nearly phase-pure state and is less susceptible to evaporative-loss of the stabilising cation. In the research described in this paper, the properties of a nearly phase-pure, dense, S-phase ceramic and its microstructural features have been examined for the Ba-stabilised variant, with a view to further improvements in microstructural design.

2. Experimental

High-purity (>99%) commercial powders, used to synthesise the S-phase ceramic were $BaCO_3$ (Aldrich), Si_3N_4 (Ube grade SNE10), AlN (Starck grade C) and Al_2O_3 (Alcoa). Appropriate amount of the precursor powders with a targeted S-phase composition of $BaAlSi_5O_2N_7$ were ball-milled in Si_3N_4 media for 24 h using isopropyl alcohol. The dried powder mixture was hot pressed in BN-coated graphite dies using RF heating at higher temperature in the range 1600–1750 °C for 2 h in nitrogen environment. The densification was monitored with a displacement transducer attached to the hot press ram. Supplementary experiments, to study the reaction/densification mechanisms, were conducted on the mixed powders, heated in nitrogen in DTA equipment, using the quartz transition as a temperature reference.

The density of hot-pressed specimens, measured by an Archimedean method, was >97% of the theoretical value for all sintering temperatures. X-ray diffraction (XRD) was used for phase identification and microstructural analysis was conducted using SEM (JEOL 6100) and transmission electron microscope (TEM) (JEOL 2000 FX) equipped with energy dispersive X-ray analysis spectrometers (EDS).

For mechanical property measurements, diamond cut and smoothly polished sections were indented with a Vickers pyramid at 50 N load (according to ASTM E384). The hardness of the hot pressed samples was determined from the indent diagonal measurements on the SEM images of the indented surfaces. The indentation fracture toughness (K_c) was determined from median crack sizes around indentations, measured on SEM micrographs and using the most frequently used Anstis's formulation.[13] The elastic modulus was measured using an ultrasonic pulse-echo technique.

Table 1
Sintered density as well as mechanical properties of the newly developed Ba-containing S-Sialon ceramics, hot pressed for 2 h in nitrogen atmosphere

Hot pressing temperature (°C)	ρ (g cm^{-3})	E (GPa)	H_{V5} (GPa)	K_{IC5} (MPa m$^{1/2}$)
1600	3.62	215	8.6 ± 0.1	2.4 ± 0.2
1700	3.63	228	12.7 ± 0.4	3.9 ± 0.3
1750	3.65	212	12.5 ± 0.4	3.7 ± 0.1

3. Results and discussion

3.1. Microstructural development

The density data as well as mechanical properties of the hot pressed S-Sialon ceramics are presented in Table 1. It is noted that the sintered density marginally varies with hot pressing temperature, with highest sintered density of 3.65 g cm^{-3} measured after hot pressing at 1750 °C for 2 h. The monitored ram displacement during hot-pressing, together with differential thermal analysis (DTA) data (Fig. 1a), indicates an initial component reactivity and associated shrinkage between 700 and 850 °C and the formation/melting of a sintering liquid (based on a Ba-aluminosilicate) above ∼1150 °C. Near theoretical density (∼3.6 g cm^{-3}) is achieved at relatively lower hot pressing temperatures and times (1600 °C/2 h), but the X-ray diffraction traces (Fig. 1b) indicate that the solution/reprecipitation reaction for S-phase recrystallisation is incomplete. The transient sintering liquid is further reduced in volume with increased temperature and time as the volume fraction of S-phase increases. The X-ray traces also show a trace amount of β′-Sialon and the partial crystallisation of residual liquid, normally to $BaAl_2SiO_6$. The acicular β′-phase and the residual silicate glass phase in a S-Sialon ceramic (hot pressed at 1700 °C/2 h) are visible in back-scattered SEM images (Fig. 2) in darker and lighter contrast, respectively, compared with the S-phase which has an intermediate Ba content, which dominates the atomic number contrast. Extensive phase analysis (semi-quantitative) study using SEM–EDS indicates that the hot pressed microstructure contains (4–5%) residual glass and (6–8%) α/β-Si_3N_4, besides the characteristic S-phase.

In order to illustrate the major features of the microstructural evolution, S-Sialon ceramic, hot pressed at 1700 °C is selected for detailed TEM study. This selection is primarily done because of the fact that the sample, hot pressed at 1700 °C contains lowest amount of intergranular glass phase. Bright field TEM images reveal a microstructure dominated by a contiguous array of elongated platelet crystals of S-phase with a minor intercrystalline liquid residue in triple junction channels (Figs. 3 and 4). The presence of fine β′ crystals within the S-phase suggests that they are formed early in the sintering reaction and subsequently act as heterogeneous nucleants for the main phase. The analysis of the selected area diffraction pattern (SADP) suggests that the S-phase crystals possess a preferred growth in the [0 0 1] orthorhombic axis with primary facets parallel to (0 1 0) and (1 0 0) planes (Fig. 3). TEM–EDS analysis indicates that an average composition for S-phase within a typical 1700 °C sin-

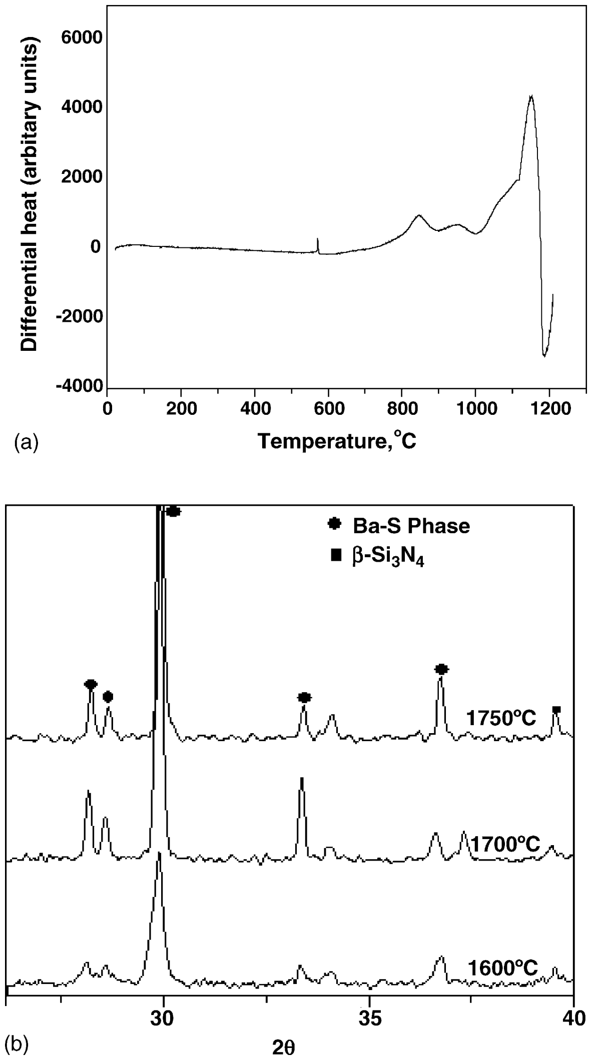

Fig. 1. DTA data obtained with Ba-containing S-Sialon starting powders with quartz as reference material (a). XRD spectra showing S-phase crystallisation over a range of hot pressing temperature (b). The sintering time at each temperature is 2 h.

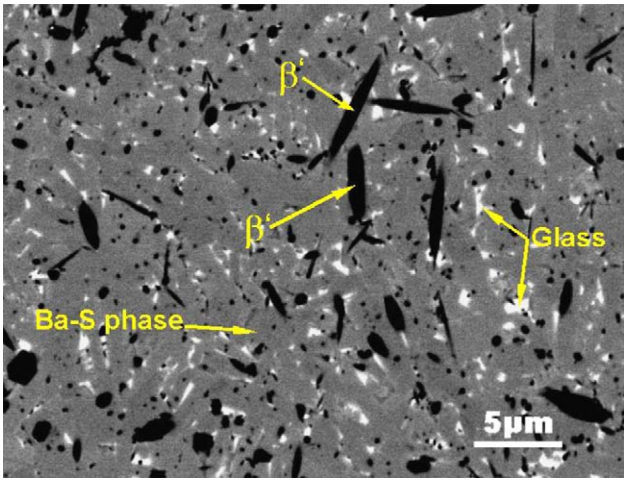

Fig. 2. Back-scattered electron (SEM) image showing minor phases (β′ and residual glass) in dark and light contrast relative to the major S-phase in a S-Sialon ceramic, hot pressed at 1700 °C for 2 h.

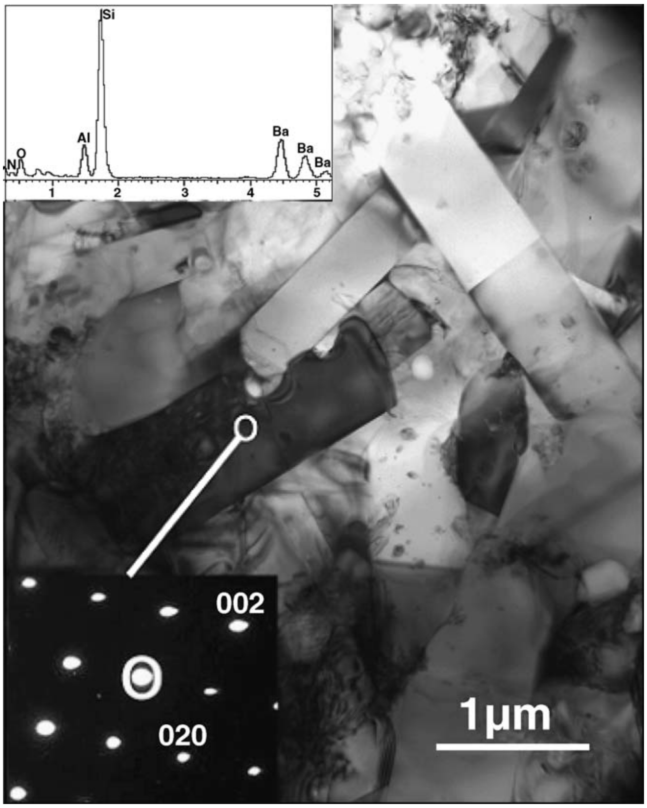

Fig. 3. Bright field TEM image illustrating the elongated platelet morphology of S-phase in a S-Sialon ceramic, hot pressed at 1700 °C for 2 h. A selected area diffraction pattern as well as EDX spectra taken from the S-phase is also shown in insets.

tered specimen is $Ba_2Si_{12-x}Al_xO_{2+x}N_{16-x}$ ($x = 2.0 \pm 0.2$), but hot-pressings with larger variations in x, in the initial powder mixture, are possible. A trace of α-Si_3N_4 must arise from unreacted and entrapped particles from the initial starting powders, since Ba does not stabilise the α′-Sialon structure. The morphology of S-phase crystals has been analysed via comparison of images with electron diffraction patterns. Many of the crystals retain their facetted form, characteristic of growth into a liquid phase. The presence of the residual glass phase is clearly visible in Fig. 4a. TEM–EDS analysis of the glass, as shown in Fig. 4b, indicates that the glass phase is Ba-rich aluminosilicate. Also, the possible composition range of the triple pocket glass is shown in Fig. 5.

Nearly all S-phase crystals contain stacking-faults, imaged with characteristic fringe contrast, which have a weak crystallographic preference (Fig. 4). We believe that the stacking faults result from growth accidents, corresponding to relative translation of crystal components by a partial lattice translation, and terminate either on partial dislocations or on the crystal surface. They are likely to be anti-phase boundaries (APBs), which are low energy faults either within the N/O network or the cation sub-lattice alone. The bright field TEM images revealing the defect structure in S-Sialon ceramic are shown in Figs. 6 and 7. The network of partial dislocations, appearing in fringes, can be noted in Fig. 6. In most of the investigated S-Sialon grains, closely spaced APBs were also observed (Fig. 7). These APBs

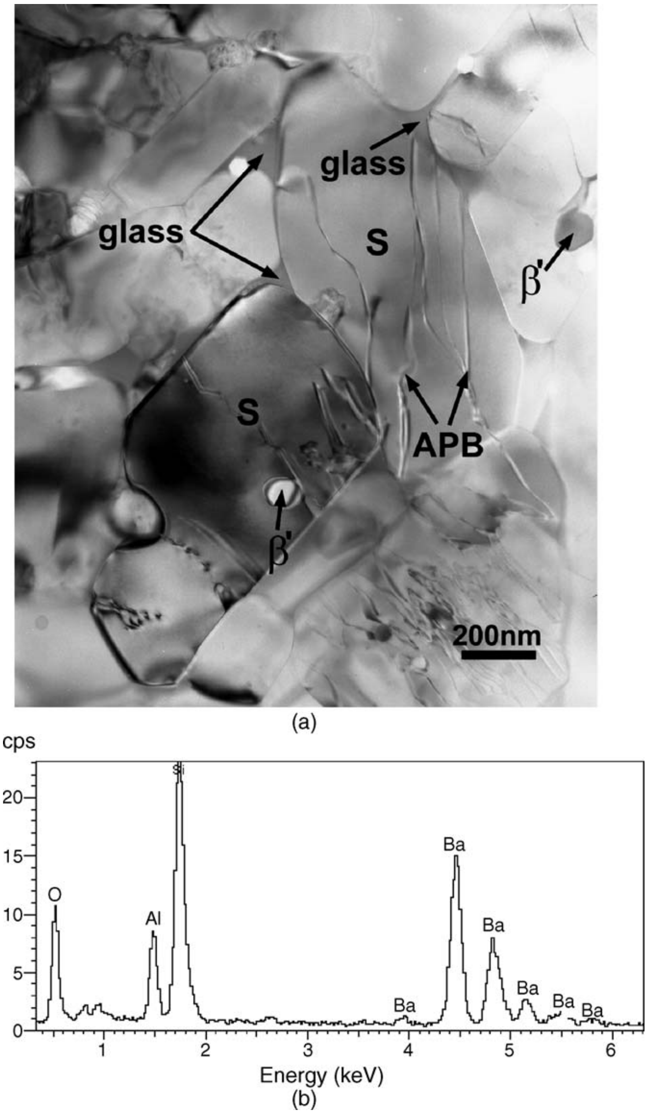

Fig. 4. Bright field TEM image of S-phase crystals with residual intercrystalline glass, included β′ and anti-phase boundaries in a S-Sialon ceramic, hot pressed at 1700 °C for 2 h (a). TEM–EDS analysis of the glass phase is also shown (b).

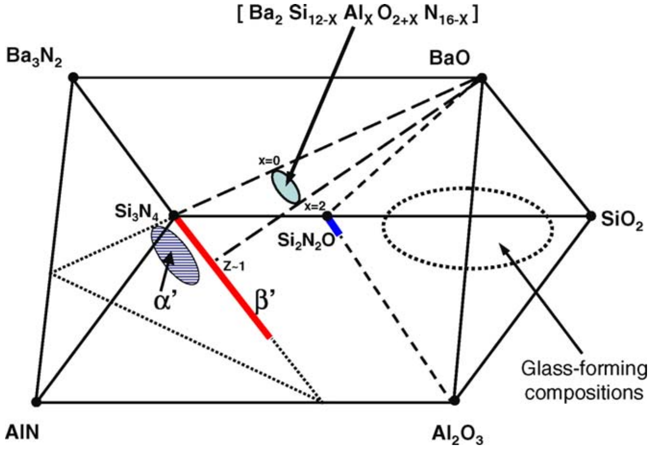

Fig. 5. Phase equilibria of interest showing the possible composition range of the residual liquid phase, formed at the triple pocket during hot pressing of the investigated S-Sialon ceramic.

Fig. 6. Bright field TEM image of S-phase revealing the presence of a network of partial dislocations in a S-Sialon ceramic, hot pressed at 1700 °C for 2 h.

occasionally extend between grain facets; whereas on some instances, APBs were observed to terminate on partial dislocations. Detailed TEM–SADP analysis of S-phase indicates that the orthorhombic unit cell is characterised by cell dimensions of $a = 8.23$ Å, $b = 9.65$ Å, $c = 4.91$ Å, which further suggests that dislocation Burgers vectors will be large. The 3D-tetrahedral linkages indicate that there are no weakly bonded planes of potential shear, but the density of these linkages is smaller than in α′- or β′-Sialon phases. The shortest lattice translations in Ba-S-Sialon are of the type $(a/2)\ \langle 1\,1\,1\rangle$ and the lowest density of tetrahedral linkage is across planes of type (1 1 0), which contain the potential Burgers rector, such that anticipated slip systems are $\{1\,1\,0\}\langle 1\,1\,1\rangle$.

3.2. Mechanical properties

The basic mechanical properties (modulus, hardness and toughness) of Ba-containing S-Sialon ceramic, hot pressed at varying temperatures have been measured. Table 1 presents the summary of the mechanical property data recorded with the hot pressed S-Sialon ceramics. The elastic modulus, obtained with a pulse-echo technique at ultrasonic frequencies, provides a value in the range 210–230 GPa, with the highest modulus of 228 GPa measured with the ceramic hot pressed at 1700 °C. This is less than for β′- or α′-Sialons, not only because of the comparatively unrefined microstructure, but mainly due to the anticipated reduction in structural rigidity associated with lack of continuity in tetrahedral SiAl(O,N)$_4$ linkage associated with the large interstices occupied by the more weakly bound Ba cation.

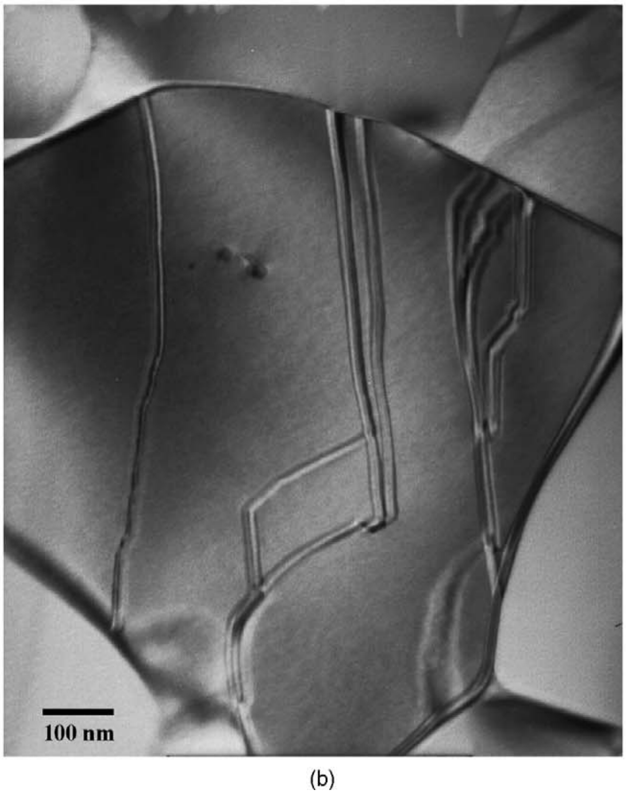

Fig. 7. Bright field TEM images revealing the details of the defect structure within a S-phase grain in a S-Sialon ceramic, hot pressed at 1700 °C for 2 h. The defect structure is characterised by APBs (formed due to fault in framework structure), infrequently observed to terminate at the partial dislocation (a) and also by the presence of APBs, extending between the facets of ‘S’ crystal.

For samples hot pressed at 1700 °C or higher temperature, the indentation (Vickers) hardness has a mean value of 13 GPa but, as in other Sialon ceramics, is sensitive to residual intercrystalline glass volume. The measured low hardness (∼9 GPa) of the S-Sialon ceramic, hot pressed at 1600 °C is largely due to the presence of significant amount of residual glass. The hardness property can undoubtedly be enhanced with more refined constitution and sintering cycle and may approach that of a typical β′-Sialon (16–17 GPa) as an intrinsic monophase property associated with the resistance to dislocation motion in the S-phase crystal.

Looking at Table 1, it is also clear that indentation toughness of the sample, hot pressed at 1600 °C is fairly poor (∼2 MPa m$^{1/2}$). However, the indentation toughness (K_c), measured with S-Sialon ceramics (hot pressed at 1700 and 1750 °C) using indentation cracking method, is in the range 3.5–4 MPa m$^{1/2}$. This is not an intrinsic S-phase property, but is dictated by crystal size, morphology and interface character. Dominant mechanisms for toughness-enhancement, demonstrated in β silicon nitrides and Sialons, are crack bridging and subsequent crystal ‘pull-out’. Fig. 8 presents a representative SEM image revealing the crack path-microstructure interaction in Ba-containing S-Sialon ceramic, hot pressed at 1700 °C. Considerable amount of crack deflection along the acicular shaped S-phase boundary is critically noted. Also, the contribution from crack bridging is minimal for the developed ceramic. The prerequisite for crack bridging is relatively weak intercrystalline bonding, and hence intergranular fracture is believed to be enhanced by the presence of glassy nanometer-layers, which are liquid-sintering residues.

The S-phase ceramics have similar microstructural features and especially the anisotropic growth of prismatic or platelet crystals, with preferred [0 0 1] growth axis. The interfacial character and cohesion is not well defined, but the presence of glassy residues and facetted S-phase growth morphology suggests a

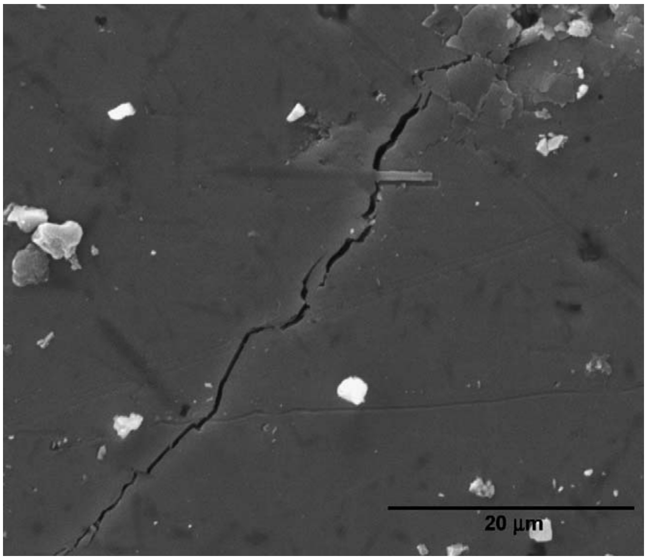

Fig. 8. SEM image showing the microstructure–crack path interaction revealing the crack deflection with little contribution from crack bridging in S-Sialon ceramic, hot pressed at 1700 °C for 2 h.

similar behaviour to β′-Sialons. There is considerable potential for enhancement of K_c by crystal coarsening with modified sintering cycles and the use of intentional β-Si_3N_4 seeding. Similar microstructural design strategies have been effective in β′-Sialon ceramics, with indentation K_c levels of ~5 MPa $m^{1/2}$ being raised to nearly 10 MPa $m^{1/2}$. There is also a possibility of fabricating β′-S-phase biphasic microstructures, which may have a property synergy, as in the earlier β′–α′ ceramics.

It is possible that S-phase Sialon ceramics may find a niche in engineering application, based on competitive low temperature properties and more economic fabrication using relatively low temperature, transient, sintering liquids. It is also feasible that moderately high temperature applications will benefit from crystallisation of sintering residues to refractory phases such as celsian. As functional ceramics, the S-phase may be a refractory, hard, matrix for partial solid solution of active ions, such as the rare earths (the partial substitution of Eu^{2+} has been reported in a Ba-S phase[11]).

4. Conclusions

Near monophasic S-Sialon ceramics in the Ba–Si–Al–O–N system is processed by hot pressing in the temperature range of 1600–1750 °C. The obtained ceramics found to be near fully dense (density 3.6 g cm^{-3}).

(a) Typical hot pressed microstructure consists of three major phases: the anisotropic platelets of 'S' phase, residual glass (4–5%) and α/β-Si_3N_4 (6–8%). TEM–EDS analysis indicates the S-phase composition to be slightly Al-rich $Ba_2Si_{12-x}Al_xO_{2+x}N_{16-x}$ ($x = 2 \pm 0.2$).

(b) The newly developed ceramics Ba-containing S-Sialon ceramics exhibit moderate hardness of ~13 GPa and modest indentation fracture toughness of ~3.5–4 MPa $m^{1/2}$, lower than typical of a ceramic with morphologically anisotropic grains contributing to bridging and pull-out mechanisms. The acoustically measured *E*-modulus is ~210–230 GPa.

(c) The sintering mechanism is based on the formation of a Ba–Al-silicate liquid around 1200 °C (DTA results), resulting in a minor (<5%) intergranular glass phase with dissolved nitrogen. The microstructure evolution during the liquid phase sintering follows the heterogeneous nucleation of the S-phase on β-Si_3N_4 in a solution-reprecipitation route.

(d) Detailed TEM analysis suggested that 'S' phase has the preferred anisotropic growth direction along the '*c*' axis of the orthorhombic unit cell and the facets of the platelets have an crystallographic orientation along (1 0 0) and/or (0 1 0) primary crystal planes.

Acknowledgements

The authors wish to thank their collaborators in University of Stockholm, in particular Dr Z. Shen, Dr M. Nygren and Dr J. Grins for discussion related to the unpublished X-ray data.

References

1. Riley, F. L., Silicon nitride and related materials. *J. Am. Ceram. Soc.*, 2000, **83**, 245.
2. Lewis, M. H., Fung, R. and Taplin, D. M. R., Indentation plasticity and fracture of Si_3N_4 ceramic alloys. *J. Mater. Sci.*, 1981, **16**, 3436–3437.
3. Lange, F. F., Relations between strength, fracture energy, and microstructure of hot pressed Si_3N_4. *J. Am. Ceram. Soc.*, 1973, **56**, 518–522.
4. Basu, B., Vleugels, J., Kalin, M. and Van Der Biest, O., Friction and wear mechanism of Sialon ceramics under fretting contacts. *Mater. Sci. Eng.*, 2003, **A359**, 228–236.
5. Thompson, D. P., Tough cookery. *Nature*, 1997, **389**, 675–677.
6. Chen, I. W. and Rosenflanz, A., A tough ceramic based on α-Si_3N_4; with a whisker like microstructure. *Nature*, 1997, **389**, 701–704.
7. Hoffman, M. J. and Petzow, G., *Tailoring of Mechanical Properties of Si_3N_4 Ceramics*. Kluwer Academic, Dordrecht, 1994.
8. Shen, Z., Zhao, Z., Peng, H. and Nygren, M., Formation of tough interlocking microstructures in silicon nitride ceramics by dynamic ripening. *Nature*, 2002, **417**, 266–269.
9. Grins, J., Shen, Z., Nygren, M. and Ekstrom, T., *J. Mater. Chem.*, 1995, **5**, 2001–2005.
10. Lewis, M. H., Reed, C. J. and Butler, N. D., *Mater. Sci. Eng.*, 1985, **71**, 87.
11. Shen, Z., Grins, J., Esmaeilzadeh, S. and Ehrenberg, H., Preparation and crystal structure of a new Sr containing Sialon phase $Sr_2Al_xSi_{12-x}N_{16-x}O_{2+x}$ ($x \sim 2$). *J. Mater. Chem.*, 1999, **9**, 1019–1022.
12. Hwang, C. J., Susnitzky, D. W. and Beaman, D. R., *J. Am. Ceram. Soc.*, 1995, **78**, 588–592.
13. Anstis, G. R., Chantikul, P., Lawn, B. R. and Marshall, D. B., A critical evaluation of indentation techniques for measuring fracture toughness: I. Direct crack measurements. *J. Am. Ceram. Soc.*, 1981, **64**, 533–538.